# EVALUATION OF SEISMICALLY ISOLATED TALL BUILDING BASED ON LONG-TERM MONITORING

**Daiki Sato [1], Yoji Ooki [2], Hitoshi Morikawa [3], Satoshi Yamada [4], Hiroyasu Sakata [4], Hiroaki Yamanaka [5], Kazuhiko Kasai [6], Akira Wada [6] and Haruyuki Kitamura [7]**

[1] *Assistant Professor, Dept. of Architecture, Tokyo University of Science, Japan*
[2] *Assistant Professor, Structural Engineering Research Center, Tokyo Institute of Technology, Japan*
[3] *Associate Professor, Dept. Built Environment, Tokyo Institute of Technology, Japan*
[4] *Associate Professor, Structural Engineering Research Center, Tokyo Institute of Technology, Japan*
[5] *Associate Professor, Dept. of Environmental Science and Technology, Tokyo Institute of Technology, Japan*
[6] *Professor, Structural Engineering Research Center, Tokyo Institute of Technology, Japan*
[7] *Professor, Dept. of Architecture, Tokyo University of Science, Japan*
*Email: daiki-s@rs.noda.tus.ac.jp, ooki@serc.titech.ac.jp, morika@enveng.titech.ac.jp, naniwa@serc.titech.ac.jp, hsakata@serc.titech.ac.jp, yamanaka@depe.titech.ac.jp, kasai@serc.titech.ac.jp, wada@serc.titech.ac.jp, kita-h@rs.noda.tus.ac.jp*

**ABSTRACT :**

Recently, the number of monitoring reports of seismically isolated building is gradually increasing. In this paper, a long-term dense monitoring system of seismically isolated tall building in Tokyo Institute of Technology is introduced. In this monitoring system, the acceleration at ground surface, 1st, 2nd, 7th, 14th and 20th floor is recorded in detail, as well as the story drift and acceleration at the floor where the base isolators are located. Using the data, the response characteristics of the building are evaluated, and these results are compared with analysis results.

**KEYWORDS:** Isolated System, Isolated Tall Building, Earthquake Observation, Wind Observation, Natural Frequency, Torsion Response

## 1. INTRODUCTION

The seismically isolated building in Japan initiated from the Yachiyo-dai-house in 1982. Recently, the number of the tall buildings having the seismically isolation system are gradually increasing in Japan. The traditional fixed based structures had many experiences of collapses or damage for the major earthquake. However, because the seismic isolated structures are new technology and these are not encountered with the major earthquake and large damage, the investigations and researches of the response characteristic about the full-scale isolated structures are not sufficient yet.
In 2005, 20-story seismically isolated building was constructed in Tokyo Institute of Technology Suzukake-dai Campus. As the one of the main themes of the Center for Urban Earthquake Engineering (CUEE) in Tokyo Institute of Technology, which is the 21st Century COE program, a long-term dense monitoring of this building is carried out. The observed data are used to define the characteristic of the isolated tall building including the ground motion. In this paper, a long-term dense monitoring system of this building is presented. The dynamic response characteristics of the tall isolated building are evaluated based on the long-term monitoring results are discussed.

## 2. SEISMICALLY ISOLATED TALL BUILDING AND MONITORING SYSTEM

### *2.1. Seismically Isolated Tall Building*

Figure 1 illustrates the elevation of the 20-story seismically isolated building, and it is called as "J2-building" in this paper. Figure 2 shows the plan of the isolation floor of J2-building. The

foundation and 1st floor of this building are RC structure. The other floors are hybrid with steel beams and CFT columns.

In the isolated floor of this building, several types of dampers are installed. The 1,200$\phi$ rubber bearings with conical spring (Figure 3 (a)) are installed in the position A as shown in Figure 2. In the position B, the steel dampers (Figure 3 (b)) are attached, and the 1,100 $\phi$ rubber bearing with the steel dampers (Figure 3 (c), (d)) are installed in the position C and D, respectively. In the position E, the 1,000kN oil dampers (Figure 3 (e)) are installed.

So called Mega-Braces (□ - 500mm x 160mm x 19 to 32mm) are installed on the both sides of building because the horizontal stiffness is necessary to maintain the seismic isolation effects. Because this building is very slender shape with the height of 91m and aspect-ratio of 5, tensile force in the rubber bearing becomes a critical design problem. If this tall seismic isolated building suffers a major earthquake, the large up-lift forces may develop at the multi-layer rubber bearings due to the tensile force cause by the large overturning moment. To avoid the large tensile forces, the bearings are enabled to do up-lift in this isolated system (Figure 3 (a)).

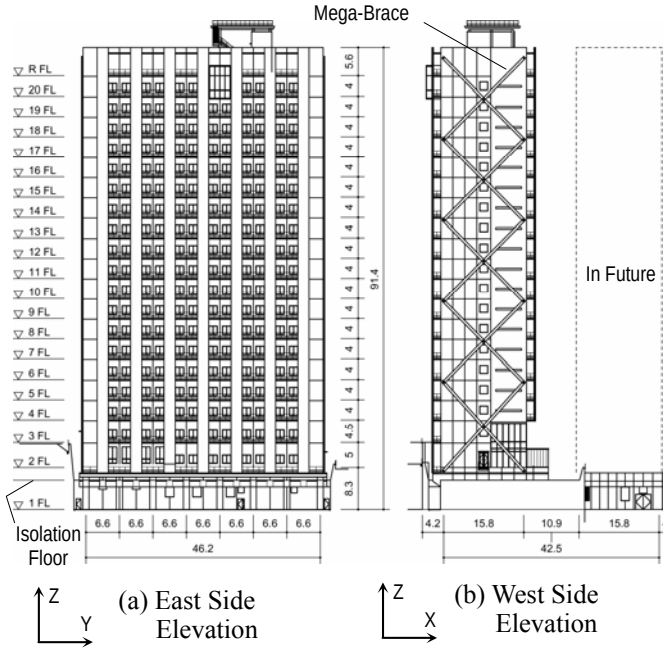


(a) East Side Elevation (b) West Side Elevation

Figure 1 J2-building (unit: m)

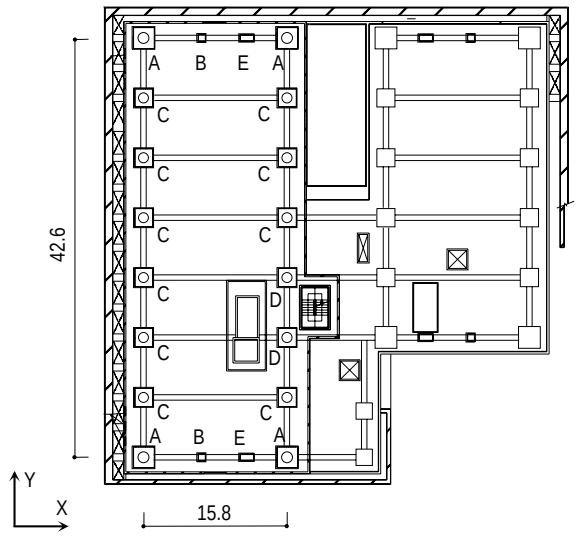


Figure 2 Seismic Isolation Floor (unit: m)

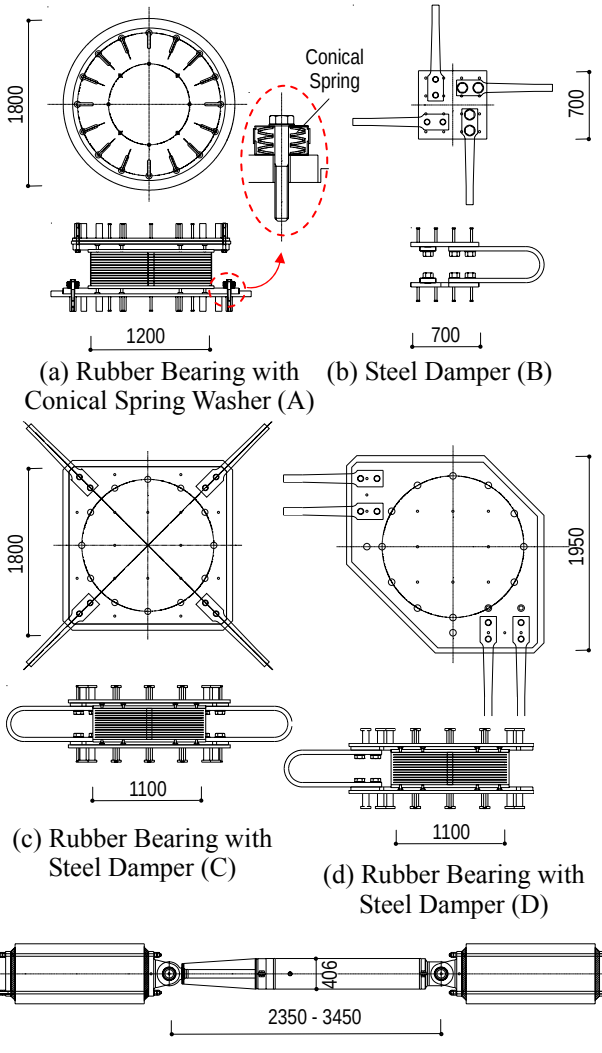


(a) Rubber Bearing with Conical Spring Washer (A)

(b) Steel Damper (B)

(c) Rubber Bearing with Steel Damper (C)

(d) Rubber Bearing with Steel Damper (D)

(e) Oil Damper (E)

Figure 3. Rubber Bearing & Damper (unit: mm)

### *2.2. Monitoring System*

Figure 4 shows the monitoring system and the list of the sensors are indicated in Table 1. In this long-term monitoring system, the accelerometers are placed on the ground surface, 1st, 2nd, 7th, 14th, 20th floor. This instrument is broad, thus the time history of displacement can be computed by numerical integration. The displacement transducers are installed to measure the displacement of the isolation devices. To measure the large and/or small inter-story displacement in the isolated story level between 1st and 2nd floors, a trace recorder is used in combination with the other measurement devices. The trace recorder is fixed to the steel beam at the bottom of the superstructure while the stainless steel board, on which the behavior of the isolated story is drawn, is fixed to the concrete slab at the top of the substructure. The strain gages are installed at the columns and the Mega-Braces. Oil damper force and deformation are measured. To measure the up-lift of the isolator as shown in Figure 3(a), the displacement transducers and the video camera are placed.

Output voltage of accelerometers, displacement transducers and strain gages are A/D converted by data loggers installed at each floor, transmitted to data servers through a LAN, and recorded continuously. The clock on data server is set using a GPS signal data on each data logger via the LAN.

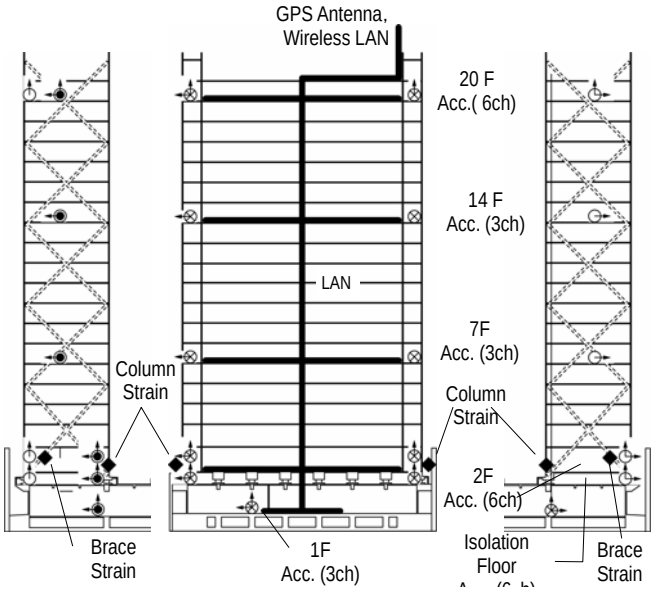


(a) Elevation

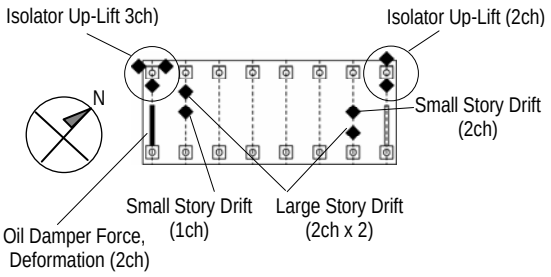


(b) Plan of Isolation Floor

Figure 4 Monitoring System

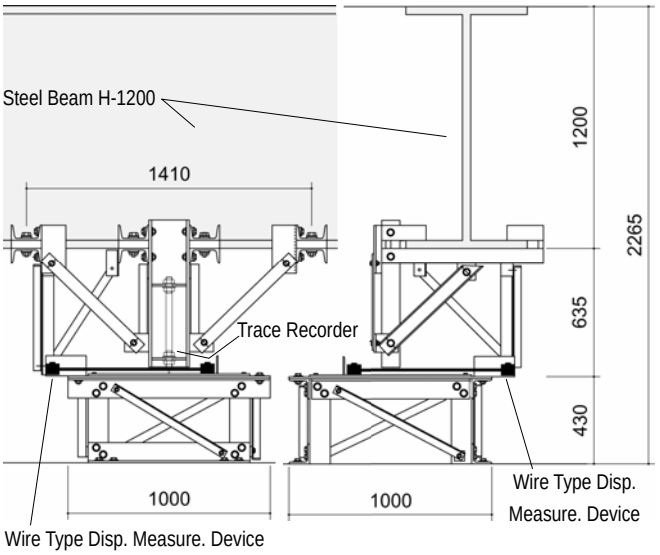


Figure 5. Measurement Device for Large Story Drift in Isolated Story (unit: mm)

Table 1 List of the Sensors

| Floor | Item | Capacity | Sensitivity |
|---|---|---|---|
| 7, 14, 20F | Acc. | 2G | 1 μG |
| | Column, Brace Strain | (Strain Gauge) | 1 μstrain |
| Isolation Floor | Acc. | 2G | 1μG |
| | Small Story Drift | ±100 mm | 0.05 mm |
| | Large Story Drift | ±500 mm | 0.5 mm |
| | Drift Trace | - | - |
| | Damper Force | (Strain Gauge) | 1 μstrain |
| | Damper Deformation | 1000mm | 0.5mm |
| | Isolator Up-Lift | 50mm (Video) | 0.03mm - |
| 1F | Acc. | 2G | 1 μG |
| Ground | Acc. | 2G | 1 μG |

## 3. RESPONSE CHARACTERISTICS

### *3.1. Observed Earthquake-induced Response*

After installing this monitoring system, some earthquakes-induced responses of the isolated building have been measured. This paper summarizes two huge observed earthquake-induced response, which are the Chiba Hokuseibu Earthquake on July 23, 2005 and the Miyagi-ken Oki Earthquake on August 16, 2005.

Figure 6 shows the recorded acceleration data at 1F and 20 F during the Chiba Hokuseibu Earthquake. Likewise, Figure 7 illustrates the observed acceleration record at 1st and 20th floor during the Miyagi-ken Oki Earthquake. It is recognized that the vibrations of 20th floor continues while the ground motion decreases sufficiently, especially in Miyagi-ken Earthquake as shown in Figure 7.

Figure 8(a), (b) respectively plot the maximum acceleration and absolute displacement response distribution of J2-building. These maximum displacements are calculated by the numerical integration from the acceleration data using band-pass filter from 0.1Hz to 30Hz. As seen in Figure 8, the response of acceleration and displacement both are concentrated in the isolated floor.

The isolated story drift traces during the Miyagi-ken Oki Earthquake are shown in Figure 9(a), (b). These traces are obtained from the trace recorders as shown in Figure 5 in the position SW and NE (See Figure4). Figure 10(a), (b) show the comparison of the isolated story drift during the Miyagi-ken Oki Earthquake obtained from the small inter-story device and the numerical integration of the acceleration time history. As shown in Figure 10, these are almost identical, it is consequently indicate that these measurement devices are accurate. As shown in Figure 9 and 10, the isolator devices are deformed 11.1mm to X-direction and 8.8mm to Y-direction, and these are the elastic range ($\leq$ 31.7mm) of the steel damper installed in the isolated floor.

Figure 11(a), (b) respectively depict the power spectrum density of the 20th floor X-direction and Y-direction acceleration during the Chiba Hokuseibu Earthquake. As can be seen from Figure 11, 1st and 2nd mode frequency of X-direction obtained from the peak of the power spectrum density are 0.39Hz and 1.19Hz, respectively. Likewise, 1st and 2nd mode frequency of Y-direction are 0.42Hz and 1.31Hz, respectively.

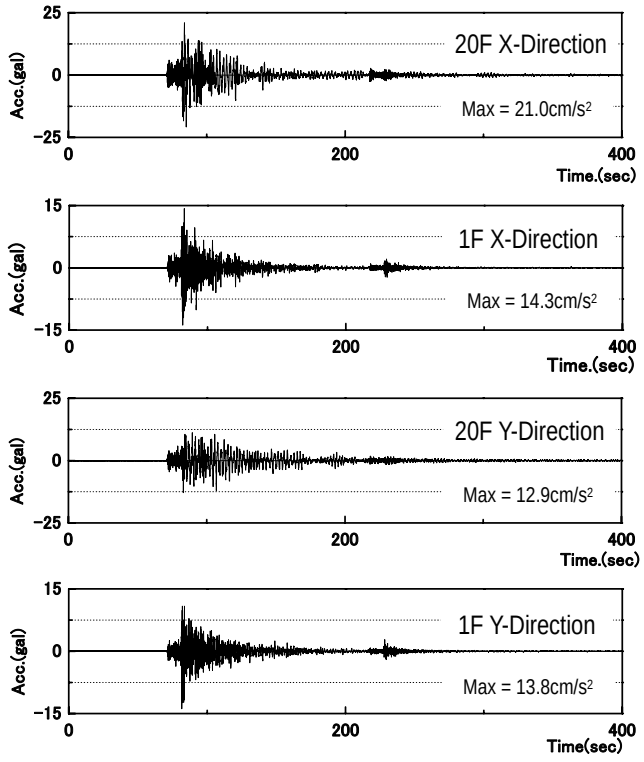


Figure 6 Acceleration Time History (Chiba Hokuseibu EQ.)

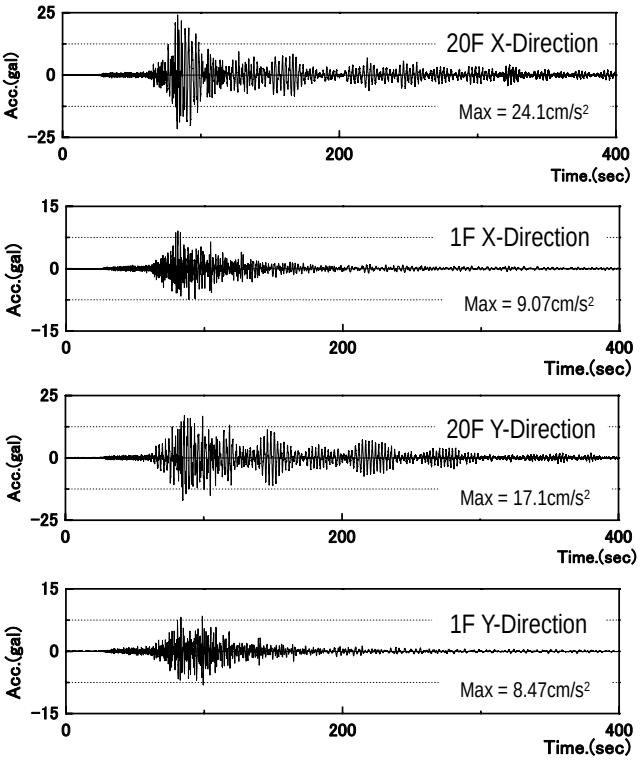


Figure 7 Acceleration Time History (Miyagi-ken Oki EQ)

Likewise, Figure 12(a), (b) illustrate the power spectrum density of the 20th floor X-direction and Y-direction acceleration during the Miyagi-ken Oki Earthquake, respectively. 1st and 2nd mode frequency of X-direction are, respectively, 0.41Hz and 1.15Hz, and those of Y-direction are 0.43Hz and 1.22Hz, respectively. These 1st mode frequencies are low as compared with the analysis results of status fixing the isolator which are calculated by Kikuchi (2005), (See Table 2).
From the results of the calculated displacement by using the two types of the band pas filters range, which, respectively, are from 0.3Hz to 0.5Hz and from 1Hz to 2Hz, respectively, it is identified that the responses around the two peaks are the sway vibration.

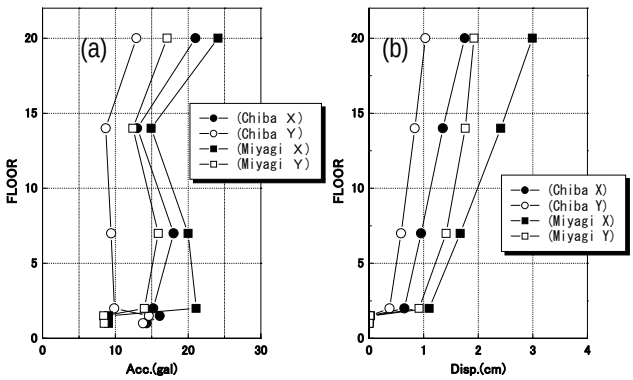


Figure 8 Maximum Response (Earthq.):
(a) Acceleration, (b) Displacement

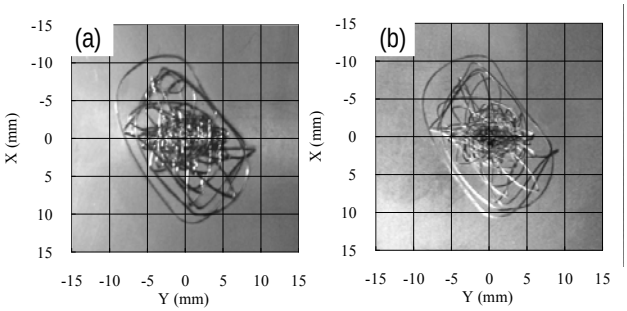


Figure 9 Drift Trace Obtained from Trace Recorder (Miyagi-ken Oki EQ.): (a) SW, (b) NN

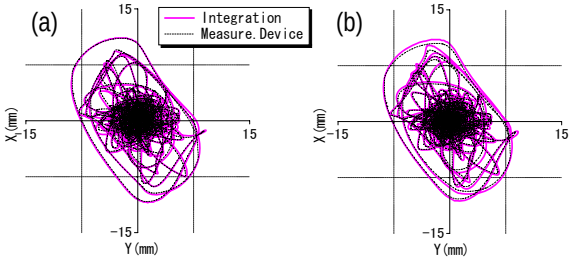


Figure 10 Comparison of Drift Trace Obtained from Integration and Measurement Device (Miyagi-ken Oki EQ.): (a) SW, (b) NN

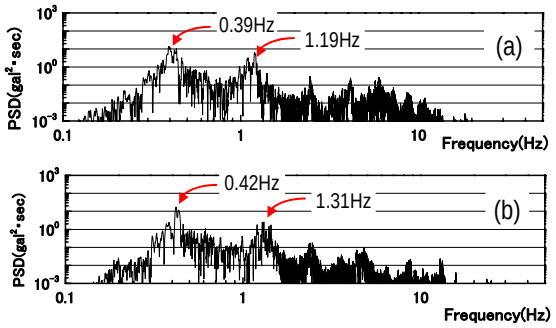


Figure 11 20F Acc. PSD (Chiba Hokuseibu EQ.):
(a) X-direction, (b) Y-direction

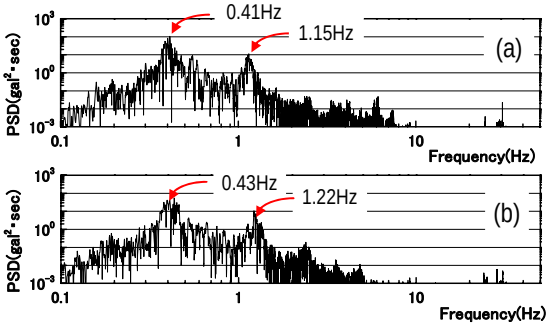


Figure 12 20F Acc. PSD ( Miyagi-ken Oki EQ.):
(a) X-direction, (b) Y-direction

### *3.2. Characteristic of Natural Frequency and Damping Ratio*

The 1st mode natural frequency and damping ratio of this isolated building are estimated from about 300 observed earthquake induced response records. Figure 13(a), (b), respectively, show the characteristic of natural frequency of X and Y-direction, and Figure 14(a), (b) illustrate the characteristic of damping ratio of X and Y-direction, respectively, and the horizontal axes of these Figures express the root mean square (RMS) of

top floor acceleration response. These results of the natural frequency and damping ratio are calculated by using the curve fit method of the frequency transfer function which is obtained from 1st floor to 20th floor acceleration records (20F/1F), and 2nd floor to 20the floor acceleration records (20F/2F), respectively. Figure 13 show that the natural frequency decrease when the response RMS increase, and it is recognized that the natural frequency of this isolated building have the response amplitude dependency. Especially, the results obtained from 20F/1F transfer function decrease compared with the results calculated from 20F/2F transfer function because the isolators are deformed in large response case. In other hand, as can be seen in Figure 14(a), (b), since the damping ration vary widely, it is difficult to identify the damping ratio.

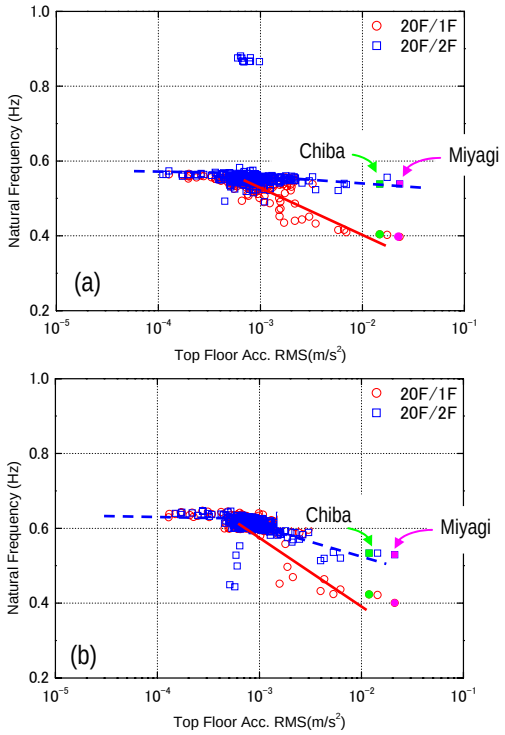


Figure 13 Characteristic of Natural Frequency: (a) X-direction, (b) Y-direction

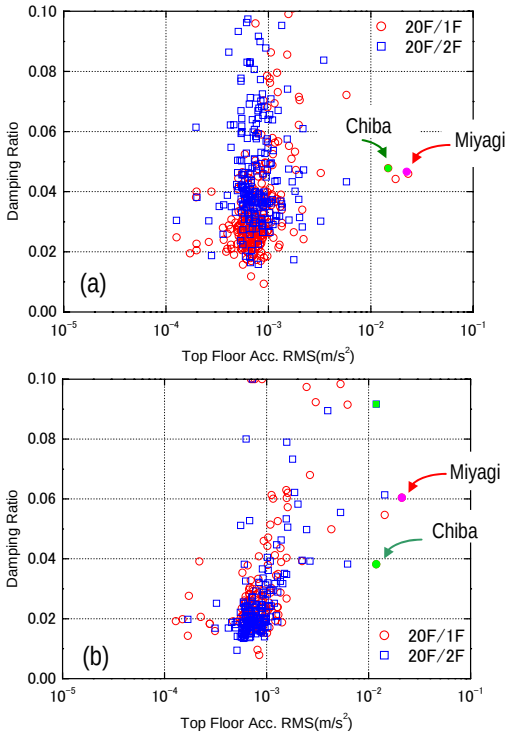


Figure 14 Characteristic of Damping Ratio: (a) X-direction, (b) Y-direction

### *3.3. Observed Wind-induced Response*

Figure 15(a), (b), respectively, show the wind-induced maximum acceleration and absolute displacement response of the 20th floor on Mar. 17 and 19 in 2005, respectively. These maximum displacements are computed by numerical integration from the 10 minute acceleration data using the band-pass filter from 0.1Hz to 30Hz. In case of the wind response, the isolators are scarcely deformed.

Figure 16(a), (b) show the power spectrum density X and Y-direction wind-induced response acceleration of the 20th floor on Mar. 17, respectively. Figure 17(a), (b) depict the power spectrum density of the 20th floor X and Y-direction wind-induced response acceleration on Mar. 19, respectively.

In X-direction power spectrum density as shown in Figure 16(a) and 17(a), there are two peaks of less than 1Hz. However, as can be seen from Figure 16(b) and 17(b), the power spectrum of density of Y-direction has only one peak which is less than 1 Hz.

From the results of the calculating X-direction displacement by using the 0.4Hz to 0.6Hz band pass filter, it is found that the responses in this range are the sway vibration. However, in case of using the band pass filter from 0.4Hz to 0.6Hz, the torsion vibrations are recognized.

Because the isolators are hardly deformed in case of the wind-induced response, 1st mode frequency during the

wind response is higher than that 1st mode frequency during the earthquake-induced response that the isolator is deformed. The comparison of natural frequency between observed data and the analysis (Kikuchi, 2005) is indicated in Table 2.

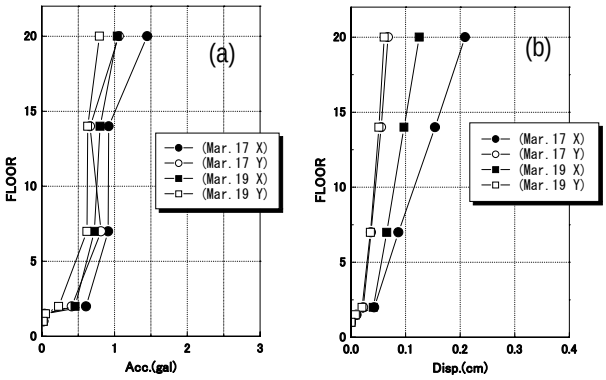


Figure 15 Maximum Response (Wind):
(a) Acceleration, (b) Displacement

Table 2 Comparison of Natural Frequency

| | Direction | Sway | Tortion |
|---|---|---|---|
| Chiba Hokusei-bu (Earthq.) | X | 0.39Hz | - |
| | Y | 0.42Hz | - |
| Miyagi-ken Oki (Earthq.) | X | 0.41Hz | - |
| | Y | 0.43Hz | - |
| Mar. 17 (Wind) | X | 0.49Hz | 0.78Hz |
| | Y | 0.57Hz | - |
| Mar. 18 (Wind) | X | 0.49Hz | 0.87Hz |
| | Y | 0.60Hz | - |
| Analysis (Isolatro Fixed) | X | 0.46Hz | - |
| | Y | 0.40Hz | - |
| Analysis ($\gamma$ = 50%) | X | 0.28Hz | - |
| | Y | 0.26Hz | - |

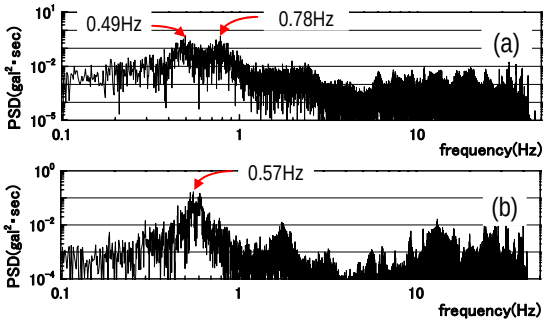


Figure 16 20F Acc. PSD (Mar. 17, Wind):
(a) X-direction, (b) Y-direction

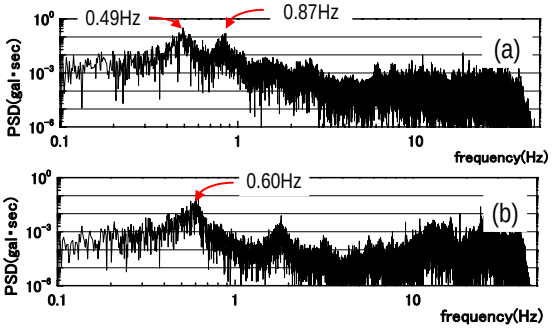


Figure 17 20F Acc. PSD (Mar. 19, Wind):
(a) X-direction, (b) Y-direction

### *3.4. Torsion Vibration of Wind-induced Response*

In case of the wind-induced response, not only the sway but also the torsion vibration is identified. In this section, the torsion vibration is focused. Figure 18(a), (b) show the torsion ratio $\alpha_\theta$ and the center of torsion, respectively. These are obtained from the ensemble average using thirteen data. The torsion ratio $\alpha_\theta$ is calculated as follows,

$$\alpha_\theta = \frac{\sigma_{\theta X}}{\sigma_X} \tag{3.1}$$

where, $\sigma_{\theta X}$ = the standard deviation of the torsion response of X-direction, $\sigma_X$ = the standard deviation of the X-direction response. The center of the torsion is obtained from the method suggested by Arakawa (2005). This method is explained briefly as follows: Firstly, the time history of the torsion response is calculated by using two points X-direction data and the distance of two points. Secondly, the natural frequency of the torsion response is obtained from the peak of the power spectrum density of the calculated torsion response. Next, each of the torsion components included in X-direction's response at the natural frequency are estimated from two points X-direction power spectrum density, respectively. Then the center of the torsion is obtained by using the distance of two points and the ratio of torsion components.

As can be seen from Figure 18(a), in North side (N) on Mar. 17, the torsion vibration components included in X-direction response of 7-20th floor and 2nd floor are about 60% and 42%, respectively. However, in the

South side (S), the characteristic of the torsion ratio are different from North side. The torsion components of 7-20th floor are 30-40%, and the torsion component of 2nd floor is 65%. In addition, the torsion responses on Mar. 17 and 19 show the different property. These differences may be caused by the wind direction, wind force and so on. However to clear these reasons, it calls for further investigation.
From what has been discussed above, the torsion vibration cannot be neglected to evaluate wind-induced response of the isolated tall building.

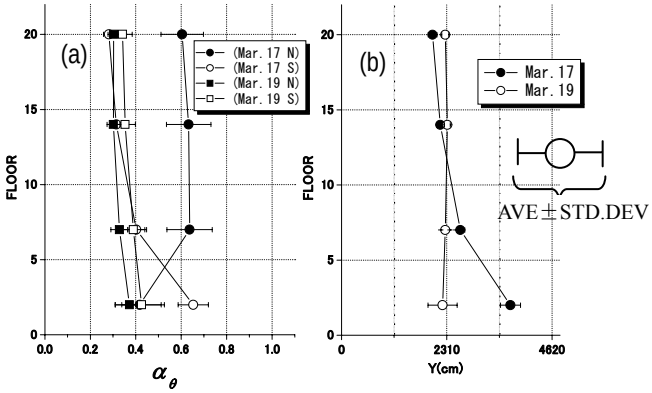


Figure 18 Torsion Response (Wind):
(a) Torsion Ratio, (b) Center of Torsion

## 4. CONCLUSIONS

A long-term dense monitoring system of the seismically isolated tall building in Tokyo institute of technology is presented in this paper. Based on the observed data obtained from earthquake and wind-induced response, the response characteristics of the building are evaluated. 1st mode natural frequency of wind response is higher than that of earthquake-induced response. It is recognized that the torsion vibration occurs only in wind response, and cannot be ignored in evaluating for the wind-induced response of the isolated tall building.

***Acknowledgements:***
This paper is the part of the results of joint-research project by the 21st Century COE program, the Center for Urban Earthquake Engineering (CUEE) in Tokyo Institute of Technology and Kitamura Lab., Tokyo University of Science.

## REFERENCES

Kikuchi, T., Fujimori, S., Takeuchi, T., and Wada, A. (2005), "Design of High Rise Seismic Isolated Steel Building with Mega-Bracing System, *Journal of Technology and Design*, Architectural Institute of Japan, No20, 217-222, Dec. (in Japanese)
Ooki, Y., Yamashita, T., Morikawa, H., Yamada, S., Sakata, H., Yamanaka, H., Kasai K., and Wada, A. (2005), Concete Approach on Long Term and Dense Monitoring System of Seismically Isolated Tall Building, *Journal of Technology and Design*, Architectural Institute of Japan, No21, 73-77, Jun. (in Japanese)
Arakawa, T., and Yoshise, S. (2005), A Study on the Evaluate on Vibration Characteristics and Amplitude Dependences for a Steel Building Based on Measuring Data, *Journal of Technology and Design*, Architectural Institute of Japan, No22, 157-162, Dec. (in Japanese)